DEVELOPMENT OF A HIGHLY ACCURATE INTERPOLATION METHOD FOR MESH-FREE FLOW SIMULATIONS I. INTEGRATION OF GRIDLESS, PARTICLE AND CIP METHODS

NOBUATSU TANAKA*

Nuclear Engineering Laboratory, Toshiba Corporation, 4-1 Ukishima-cho, Kawasaki-ku, Kawasaki, Kanagawa 210-0862, Japan

SUMMARY

A simple, efficient, flexible and accurate interpolation method, CIVA, is introduced for use with mesh-free methods for flow simulations. The method enables mesh-free cubic interpolation with the local co-ordinate system, such as volume and area co-ordinates, by utilizing the concept of the CIP scheme and allows the development of new highly accurate mesh-free methods. The mesh-free methods integrate the gridless, particle and CIP methods since they have flexibility in the treatment of moving calculation points. For achieving high accuracy with the CIVA method, it is also important to correctly evaluate particle movement. The improvement of the evaluating algorithm is another objective of this study. The validity of the algorithms is confirmed by applying them to the convection and convection–diffusion problems. Since the CIVA-based mesh-free methods enable flexible, efficient and accurate fluid simulation, they make it possible to perform highly accurate simulations of many kinds of problems that involve complicated geometries and phenomena. Copyright © 1999 John Wiley & Sons, Ltd.

KEY WORDS: gridless method; particle method; CIP; local co-ordinates; CIVA; time marching scheme

1. INTRODUCTION

Although the finite difference method (FDM) and finite element method (FEM) are the most popular mesh-using methods in the field of flow simulations, they are of limited applicability to problems involving complex geometries or complex phenomena because the results obtained by the methods depend strongly on the mesh characteristics. Thus, generating a good mesh requires a lot of time and great care. Consequently, mesh-free methods, which do not require the construction a mesh, have been attracting the attention of fluid dynamics researchers. We can classify the mesh-free methods into two groups, The gridless (Eulerian) method and the particle (Lagrangian) method. Adopting broad definitions, by 'gridless method' we mean mesh-free flow simulation with fixed calculation points and by 'particle method' we mean mesh-free flow simulation using calculation points that move according to the flow. The concept of the gridless method utilizing least-squares approximation, which was developed for treating complex geometries, was originally proposed by Batina [1] and was subsequently

---

* Correspondence to: Nuclear Engineering Laboratory, Toshiba Corporation, 4-1 Ukishima-cho, Kawasaki-ku, Kawasaki, Kanagawa 210-0862, Japan. E-mail: nobuatsu.tanaka@toshiba.co.jp

improved by Satofuka *et al.* [2] and others. On the other hand, some particle methods for moving boundary problems have been developed by Harlow [3], Chorin [4], Monaghan [5] and Koshizuka and Oka [6]. Both the gridless method and the particle method have flexibility with respect to the calculation points, and are therefore useful for fluid problems that involve complicated geometries and complicated phenomena. Conversely, they have the drawbacks that improvement of numerical accuracy and application to high Reynolds number flow are difficult.

In the conventional gridless method, the scalar quantity around a certain point is approximated as a function, and the spatial derivatives in the governing equation are evaluated by the least-squares method. The gridless method thus causes numerical errors (numerical viscosity) in the function approximation of the least-squares method. Therefore, the increase in the number of points and the usage of high-order functions do not necessarily lead to an improvement of accuracy. In addition, since the gridless method is essentially a central difference scheme, there is also a problem with stability.

In the particle method, although the convection term is expressed by movement of calculation points (particles), data interpolation is required when particles need to be rearranged in order to cancel the heterogeneity of the particle distribution. Generally, linear (first-order) interpolation is used, but this low-order interpolation leads to generation of numerical viscosity in the same manner as in the case of the gridless method. Thus, in the conventional mesh-free technique, a major problem is the numerical viscosity produced by the function approximation or the interpolation. This problem arises because there is no suitable and highly accurate interpolation algorithm applicable to mesh-free methods.

Recently, the cubic interpolation pseudo-particle (CIP) method [7,8] has also attracted the attention of researchers. With this method it is possible to improve accuracy and stabilize the solution with the third-order interpolation using the spatial derivatives as variables. Since the CIP method is originally a rectangle or rectangular parallelepiped mesh-based method, it is difficult to apply it to mesh-free methods. First of all, as shown in Appendix A, the CIP method is a third-order scheme in terms of space accuracy, and uses a rectangular mesh. This method is less advantageous than other third-order difference schemes, such as the UTOPIA and K–K method because it requires a great deal of memory and has a high computing cost. However, if the concept of the CIP method could be made applicable to the mesh-free methods, it would be extremely useful and powerful.

An objective of this study is to develop a highly accurate (CIP-type) interpolation algorithm applicable to the mesh-free method. One of the methods of developing the algorithm is based on a triangular unit in two dimensions and a tetrahedral unit in three dimensions. In this case, we only locally compose a suitable triangle or tetrahedron (local mesh), including the target point for interpolation from calculation points when interpolation is required. However, interpolation in the local triangle using a cubic spline function becomes a problem because the amount of known information is less than that required to solve the undetermined coefficients of the complete cubic function. To solve the problem, Aoki has presented a method using the mixed second partial derivative ($\partial^2 f / \partial x \, \partial y$) as a variable [8], but the application to flow simulations raises the problems of how to calculate the variable and how to set the boundary conditions. Instead of this method, the author adopts another approach that involves reducing the number of terms of the complete cubic function without losing symmetry and without solving the linear system to determine the coefficients. The new interpolation method, which is called cubic interpolation with volume/area co-ordinates (CIVA), makes it possible to achieve highly accurate mesh-free interpolation. The method applied to two-dimensional problems was initially called cubic interpolation with area co-ordinates in a triangular unit (CAT) [9,10].

Firstly, the method and how to apply it to mesh-free methods, such as the gridless method and the particle method, are described. In the particle method, the convection terms are treated by the Lagrangian, rearrangement and interpolation (LRI) algorithm. Because the LRI algorithm with low-order interpolation yields large errors, it is necessary to combine it with a high-order mesh-free interpolation method, such as the CIVA method. As the CIVA–particle method, which combines the particle method with the CIVA method, is very flexible and independent of particle movement or rearrangement, it can integrate the gridless method, the particle method and the CIP method [10]. To confirm the validity, two examples are considered; a pure convection problem and a convection–diffusion problem.

In the mesh-free method using the CIVA method, since not only the physical quantity of a particle but also its spatial derivatives are transferred, it is necessary to move particles with sufficient accuracy. Therefore, improvement of time integration of particle movement are also performed here.

2. THE CIVA ALGORITHM

In the conventional mesh-free method, the numerical viscosity produced by the interpolation (or function approximation) becomes a serious problem because there is no highly accurate interpolation algorithm applicable to mesh-free techniques. The author therefore proposes a highly accurate interpolation method for mesh-free techniques. In mesh-free methods, interpolation of value at a target point is performed using the data of points around the position. Use of the least-squares method causes numerical error in the approximation of functions. Therefore, the increase of points and the use of higher-order functions do not necessarily lead to improvement of accuracy. That is, interpolation should generally be performed using as few points as possible. Such points form a triangle in two dimensions and a tetrahedron in three dimensions, and these forms are suitable from the viewpoint of flexibility. However, the conventional method for a triangle uses linear interpolation and causes large errors. Mesh-free interpolation is therefore performed with the third-order function using the concept of the CIP method in which scalar quantities and their spatial derivatives are taken as variables.

2.1. Formulation

Let the co-ordinate system in Cartesian co-ordinates be defined as $\mathbf{x} = (x, y)$ for two dimensions and $\mathbf{x} = (x, y, z)$ for three dimensions. In the two-dimensional case, the complete cubic function is defined as

$$f(x, y) = a_1 + a_2 x + a_3 x^2 + a_4 x^3 + a_5 y + a_6 y^2 + a_7 y^3 + a_8 xy + a_9 x^2 y + a_{10} xy^2. \tag{1}$$

When the cubic function is used to interpolate within a triangle in the same way as in the case of the CIP method, there are only nine known pieces of information for ten unknown coefficients of Equation (1). Thus, the available information is insufficient. Aoki proposed a method that compensates for the shortage of information by using mixed second partial derivatives $\partial^2 f/\partial x \, \partial y$ as variables [8]. However, when the method is applied to actual fluid simulations, the procedures for calculating the derivatives and setting up the boundary condition become a problem. Therefore, the problem will be solved by reducing the unknown coefficients. If the unknown coefficients of Equation (1) are reduced in Cartesian co-ordinates, the following problems generally arise.

(a) The symmetric property of the function collapses.
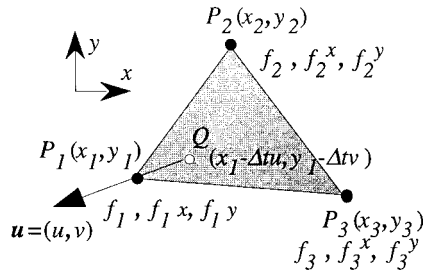
Figure 1. Two-dimensional CIVA using triangles and the upwind scheme.

(b) Simultaneous linear equations of coefficients have to be solved. This requires a large amount of calculation time.

(c) The equations become singular if the triangle takes a certain form.

These problems can be solved by using the local or natural co-ordinate system, such as area co-ordinates and volume co-ordinates, which are commonly used in the FEM field. For simplicity, the co-ordinates shown in Figure 1 are adopted and the partial differential of f with respect to x is expressed as f^x.

The area co-ordinates in two dimensions are the normalized system for triangles, and a point P within a triangle is expressed by three co-ordinate values (L_1, L_2, L_3). These co-ordinate values indicate the ratio of the area of the partial triangle shown in Figure 2 to the whole and are given by the following equation:

$$(L_1, L_2, L_3) = \left(\frac{S_1}{S}, \frac{S_2}{S}, \frac{S_3}{S} \right). \tag{2}$$

The following relation gives a 1:1 correspondence with Cartesian co-ordinates:

$$\begin{bmatrix} x \\ y \\ 1 \end{bmatrix} = \begin{bmatrix} x_1 & x_2 & x_3 \\ y_1 & y_2 & y_3 \\ 1 & 1 & 1 \end{bmatrix} \begin{bmatrix} L_1 \\ L_2 \\ L_3 \end{bmatrix}. \tag{3}$$

Here, to maintain symmetry, the cubic function corresponding to the scalar quantity in a triangle is set in the following form using the area co-ordinates:

$$\tilde{f}(L_1, L_2, L_3) = \sum_{i=1}^{3} \alpha_i L_i + d \sum_{\substack{j,k=1 \\ j \neq k}}^{3} \beta_{jk}[L_j^2 L_k + c L_1 L_2 L_3]. \tag{4}$$
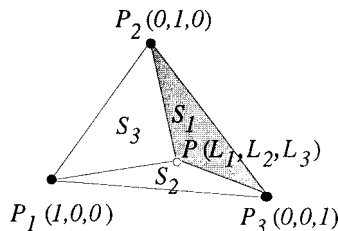
Figure 2. Area co-ordinates.
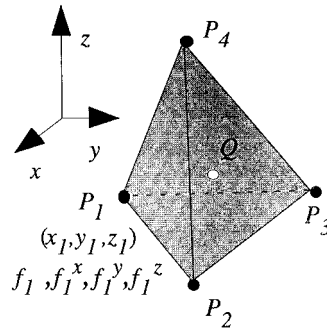
Figure 3. 3D CIVA using tetrahedrons.

This function is developed from the non-conforming shape function for plate bending analysis with the FEM [11,12]. The parameter d is the regulation parameter from the first-order to the third-order interpolation, and serves as the third-order interpolation in the case of $d = 1$ and the first-order interpolation in the case of $d = 0$. The setting up of c is an interesting problem and a subject for future investigation. The use of another calculation point and the application of the least-square approximation are among the candidate approaches to accomplish this. Here, $c = 1/2$. This is the same value as is conventionally used in the FEM plate bending analysis. This value is chosen so that the cubic function expressed by Equation (4) may give arbitrary curvatures in all the areas within a triangle (constant curvature conditions) [12]. Another reason why the value of c must be given in advance is that the term $L_1 L_2 L_3$ and the first-order spatial differential values become zero at every vertex of a triangle; therefore, the coefficients for $L_1 L_2 L_3$ cannot be determined from the known information of the vertexes. On the other hand, the rest of the unknown nine coefficients of Equation (4) can be determined independently of c and directly without solving simultaneous linear equations.

The partial differential operators with the area co-ordinates become

$$\frac{\partial}{\partial x} = \frac{y_2 - y_3}{J} \frac{\partial}{\partial L_1} + \frac{y_3 - y_1}{J} \frac{\partial}{\partial L_2} + \frac{y_1 - y_2}{J} \frac{\partial}{\partial L_3},$$

$$\frac{\partial}{\partial y} = \frac{x_3 - x_2}{J} \frac{\partial}{\partial L_1} + \frac{x_1 - x_3}{J} \frac{\partial}{\partial L_2} + \frac{x_2 - x_1}{J} \frac{\partial}{\partial L_3}, \tag{5}$$

where

$$J = (x_2 - x_1)(y_3 - y_1) - (y_2 - y_1)(x_3 - x_1). \tag{6}$$

Using these relations, the unknown coefficients of Equation (4) can be determined to be

$$\alpha_i = f_i, \qquad \beta_{jk} = f_j - f_x + (x_k - x_j)f_j^x + (y_k - y_j)f_j^y. \tag{7}$$

Therefore, by substituting the co-ordinates of arbitrary points in a triangle expressed with the area co-ordinates in Equation (4), the third-order interpolation of the scalar quantity of the point can be calculated. The derivatives can be calculated similarly by using Equation (5).

In the case of three dimensions, the CIVA method utilizes a tetrahedron for interpolation, and the volume co-ordinate is the normalized system for tetrahedrons (Figure 3). A point within a tetrahedron is expressed by the four co-ordinate values (L_1, L_2, L_3, L_4), whose co-ordinate values indicate the ratio of the volume of the partial tetrahedron to the whole. With the volume co-ordinates, the following three-dimensional cubic function in a tetrahedron can be assumed as an example.

$$\tilde{f}(L_1, L_2, L_3, L_4) = \sum_{i=1}^{4} \alpha_i L_i + d \sum_{\substack{j,k=1 \\ j \neq k}}^{4} \beta_{jk}[L_j^2 L_k + c(L_1 L_2 L_3 + L_2 L_3 L_4 + L_1 L_2 L_4 + L_1 L_3 L_4)].$$

(8)

Without solving the linear system, the coefficients α and β can be calculated independently of c as follows:

$$\alpha_i = f_i, \qquad \beta_{jk} = f_j - f_k + (x_k - x_j)f_j^x + (y_k - y_j)f_j^y + (z_x - z_j)f_j^z.$$

(9)

The parameters c and d have the same meanings as in the two-dimensional case. You must specify c in advance because the terms $L_1 L_2 L_3$, $L_2 L_3 L_4$, $L_1 L_2 L_4$, $L_1 L_3 L_4$ and the first-order spatial differential values become zero at every vertex of the tetrahedron and the their coefficients cannot be determined from the known information at the vertexes.

From the above discussion, it can be confirmed that the volume/area co-ordinates make it possible to solve the problems (a)–(c) and enable the cubic interpolation of the scalar distribution in a triangle or tetrahedron using a simple formulation.

2.2. Application to the gridless method

It is generally important in flow simulations to accurately evaluate convection effects, because the convection terms govern accuracy of the whole calculation, especially in turbulent flow. Therefore, the initial value problem of the following two-dimensional pure convection equation is considered.

$$\frac{\partial f}{\partial t} + \boldsymbol{u} \cdot \nabla f = 0,$$

(10)

where $\boldsymbol{u}$ means flow velocity, $\boldsymbol{u} = (u, v)$. The calculation points should be allotted suitably in the calculation area. The conventional gridless method solves Equation (10) by calculating the derivatives of a point by the least-squares method from the values of the surrounding points [1,2]. Therefore, the method causes numerical errors related to the function approximation of the least-squares method. Also, the increase in the number of points and the use of high-order functions do not necessarily lead to improvement of accuracy, and there is a problem with stability because the method is basically of the central difference type.

The author applies the Godunov-type upwind scheme combined with the CIVA method to estimate the convection term. The governing equations for the spatial derivatives are the same as in the CIP method and are as follows,

$$\frac{\partial f^x}{\partial t} + \boldsymbol{u}^x \cdot \nabla f^x = -\boldsymbol{u}^x \cdot \nabla f, \qquad \frac{\partial f^y}{\partial t} + \boldsymbol{u}^x \cdot \nabla f^y = -\boldsymbol{u}^y \cdot \nabla f.$$

(11)

With the same time-splitting technique as the CIP method, these equations are evaluated in the two steps of the advection phase,

$$\frac{\partial f^x}{\partial t} + \boldsymbol{u} \cdot \nabla f^x = 0, \qquad \frac{\partial f^y}{\partial t} + \boldsymbol{u}^y \cdot \nabla f^y = 0,$$

(12)

and the non-advection phase

$$\frac{\partial f^x}{\partial t} = -\boldsymbol{u}^x \cdot \nabla f, \qquad \frac{\partial f^y}{\partial t} = -\boldsymbol{u}^y \cdot \nabla f.$$

(13)
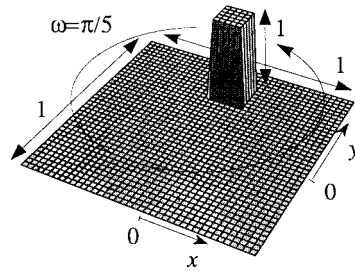
Figure 4. Pure convection problem considered for validation of the methods (initial condition of f).

In the upwind schemes, the solution of Equation (10) in the point P_1 in Figure 1 is approximated with the value of point Q on the upwind side by a time step, and the value is calculated by interpolation. The solution of Equation (10) is approximated as

$$f(\boldsymbol{x}, t + \Delta t) \approx f(\boldsymbol{x} - \Delta t\boldsymbol{u}, t). \tag{14}$$

A feature of the CIP method is that the upwind scheme is used not only for convection of the scalar quantity (Equation (10)) but also for its derivatives (Equation (12)), i.e. the advection of the spatial derivatives is also evaluated by the upwind scheme.

$$f^x(\boldsymbol{x}, t + \Delta t) \approx f^x(\boldsymbol{x} - \Delta t\boldsymbol{u}, t), \qquad f^y(\boldsymbol{x}, t + \Delta t) \approx f^y(\boldsymbol{x} - \Delta t\boldsymbol{u}, t). \tag{15}$$

The gridless method based on the CIVA method employs the same technique and calculates the scalar value and its derivative at point Q by interpolation using the cubic spline function from local triangle $P_1 P_2 P_3$ on the upstream side. Of course, choosing an inappropriately shaped triangle, such as one whose vertexes lie almost in a straight line, should be avoided because the coefficient matrix of Equation (3) becomes singular ($J \rightarrow 0$) in this case. The derivatives can be calculated similarly by a relation such as Equation (5). The author refers to the method in which the CIVA method and the gridless method are combined as the CIVA–gridless method. He evaluates the non-advection terms of Equation (13) by the Euler time marching scheme using the information in the triangle on the upstream side.

Consider the pure convection problem of a rotation field having a constant angular velocity of $\pi/5$ (rad s^{-1}) around the system center $(0, 0)$. The initial distribution of the scalar value is given in Figure 4. The distribution of f after one rotation (2π) is compared. Figure 5 is the
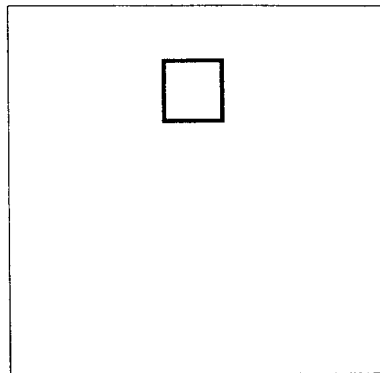
Figure 5. Exact solution.

Figure 6. Donor cell, $\Delta t = 2 \times 10^{-3}$ (second-order central difference plus 10% artificial viscosity).
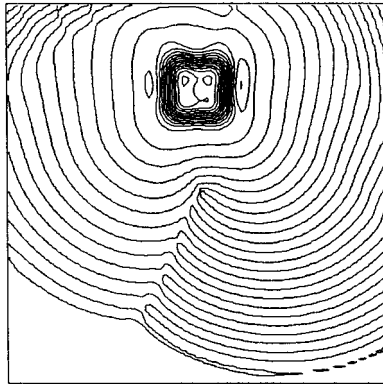
Figure 7. Third-order upwind (UTOPIA), $\Delta t = 2 \times 10^{-3}$.
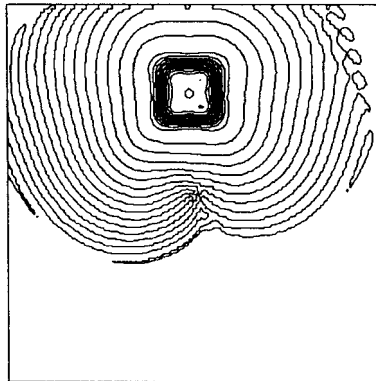
Figure 8. CIP, $\Delta t = 2 \times 10^{-2}$.

exact solution, and Figures 6–8 are the results with the finite difference method using uniform grid points. These results show that the CIP scheme has almost the same accuracy as the third-order upwind difference scheme in space when the grid points are the same. The reason why the CIP method has third-order accuracy in space is explained mathematically in Appendix A. In analyses using a rectangular mesh, the CIP method is considered to have many disadvantages, such as the increase of required memory and the amount of computation. In

other words, the CIP-type technique is considered to be particularly effective when applied to mesh-free methods, whose accuracy is otherwise difficult to improve. This is one of the reasons why the CIP-type interpolation is used for the mesh-free methods. The result obtained by the CIVA–gridless method is shown in Figure 9. The result shows that the method gives the same accuracy as the third-order upwind scheme or the CIP method when the calculation point is the same.

2.3. Application to the particle method

In the particle method the calculation points (particles) move with the flow. Since the convection term is estimated from the movement of the calculation points, the numerical viscosity is thought to be small (except for the time integration accuracy mentioned in Section 3). However, a compensation or rearrangement procedure of calculation points is generally required for the purpose of canceling the heterogeneity of particle number density [6]. In the procedure, interpolation of the physical quantity is needed. Application of a low-order interpolation, such as linear interpolation, creates significant numerical viscosity. The above mentioned CIVA method is effective in solving the problem because of the low numerical viscosity and high accuracy. The method in which the CIVA method and the particle method are combined is called the CIVA–particle method. This method is composed of three (LRI) steps. The first step consists of the movement of particles (Lagrangian step). The second step involves the particle rearrangement (rearrangement step) and the third is interpolation of the physical quantities (interpolation step). In the first step, particles move according to the fluid behavior with the scalar quantity and the spatial derivatives (Figure 11). This particle movement is also considered to be the movement of the cubic spline function according to the flow (Figure 12). The second and third steps are performed only when rearrangement is required. When particles move according to the fluid behavior, they gather or scatter at certain points. Therefore, it is necessary to compensate or rearrange particles in order to control the particle density. A simple algorithm restores the particle position at every time step. The algorithm is efficient because it allows searching of the surrounding particles at one time, but is not able to treat moving boundaries. Another use of particle rearrangement is to keep the particle number density constant [6]. After the particle rearrangement step, interpolation of the physical quantities at the new particle position is required. In the step of the CIVA–particle method, physical quantities are cubic interpolated by the CIVA method.
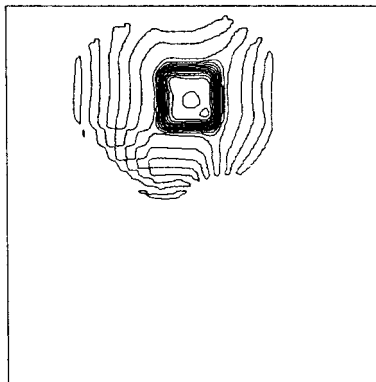
Figure 9. CIVA–gridless, $\Delta t = 2 \times 10^{-2}$.
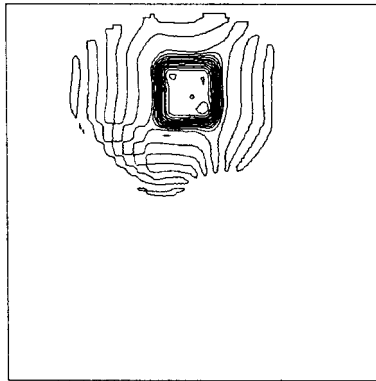
Figure 10. CIVA–PU, $\Delta t = 2 \times 10^{-2}$.

The concept of the LRI algorithm is flexible and has the following important merit. While the rearranged particle position in the gridless method is fixed to the original position and that in the particle method depends on both the original position and the flow direction, the particle position in the LRI algorithm is independent of the original position and the flow direction. In other words, the LRI algorithm is a gridless method when particles go back to each original position at every time step and is a particle method when no rearrangement is performed. Therefore, the CIVA–particle method, which combines the CIVA method, the particle method and the LRI algorithm, is able to integrate the gridless method, the particle method and the CIP method.

The author checked the validity of the CIVA–particle method by applying it to an example in which the particle position is restored at every time step. As the method requires interpolation at every time step, the effects are clearly observed. Calculation points move according to the flow with the scalar quantity and the spatial derivative quantities and then return to the original positions. The quantities in the original position are computed by the CIVA method from the values of the moved calculation points (Figure 11). In the algorithm, the scalar distribution in the local triangle, P'_1, P'_2, P'_3, shown in Figure 11, is expressed with the cubic spline function and the scalar quantity and the derivatives at point P, are calculated. The CIVA–particle method that restores the particle position at every time step is called the CIVA–particle upwind (CIVA–PU) method. With the CIVA–PU method, a calculation point can be treated as a fixed point from the viewpoint of computation in the same manner as in the CIVA–gridless method. However, the algorithm of the CIVA–PU method is superior to that of the CIVA–gridless method because it
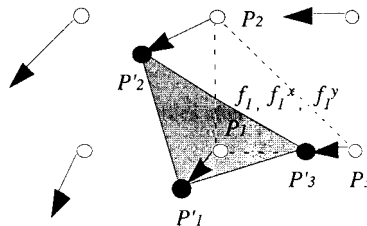
Figure 11. CIVA–particle method.
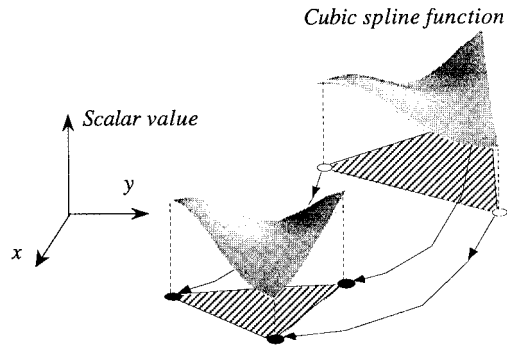
Figure 12. Explanation of CIVA–particle method using the concept of moving cubic spline.

(a) takes flow non-uniformity into consideration and
(b) accurately evaluates the target point position for interpolation.

The above mentioned CIVA–PU method was applied to the problem described in Section 2.3 with uniform calculation points. The result is shown in Figure 10. The solution with the CIVA–PU method is as accurate as those obtained by the third-order upwind (UTOPIA) scheme and the CIP scheme with finite difference discretization. Moreover, the CIVA–PU method achieved stable calculations at a time step size ten times greater than that employed in the case of UTOPIA.

Next, more quantitative comparisons are performed. For the same problem as above, the irregular points (10^4 pieces) in Figure 13 are used. The result is shown in Figure 14. For comparison, the results obtained by the Donor cell (second-order central difference plus 10% artificial viscosity) and UTOPIA (third-order upwind scheme) methods using a uniform 100×100 mesh are included. Despite the random calculation points, the obtained solution has the same accuracy as the solution obtained by UTOPIA with a uniform mesh.

The final example in this section is an interesting case that highlights the merit of the CIVA–particle method, i.e. the rearranged particle position is independent of the original position and is also free from the flow. Computation is done on calculation points that fluctuate at every time step as shown in Figure 15. The fluctuation range is $\pm 40\% \times$ (random number [0, 1]) $\times$ (original particle interval) around the original position. The result based on the particles is shown in Figure 16. In spite of this severe condition, the CIVA–particle method
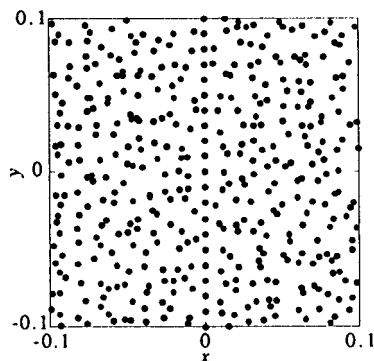
Figure 13. Some of the calculation points.
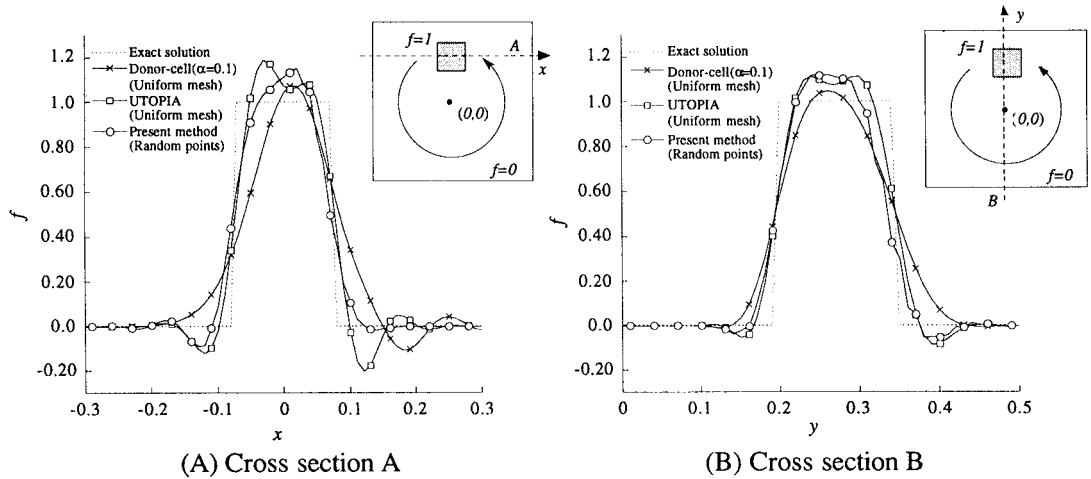
Figure 14. Comparison of scalar profiles after 2π rotation.

can give a fairly good solution. In this calculation, the deformation of the triangles used for the interpolation is also checked and Figure 17 shows one of the most deformed triangles. From the figure, the CIVA–particle method is found to be fairly robust with respect to the triangle shape.

3. IMPROVEMENT OF THE TIME MARCHING METHOD FOR PARTICLE MOVEMENT

In the particle method, convection terms are expressed by movement of calculation points (particles); therefore, accurate estimation of particle movement is required. The estimation is especially important in the case of the CIVA method because the derivatives also move with the particles. Since the accuracy of the conventional time marching or time integral schemes for the particle method is not satisfactory, the whole solution does not reach the required accuracy, even if the spatial accuracy is improved. Here, a time marching scheme is introduced to improve the accuracy of position evaluation (particle movement) in the particle method. Then, by explaining the upwind scheme in terms of movement of virtual particles, the time
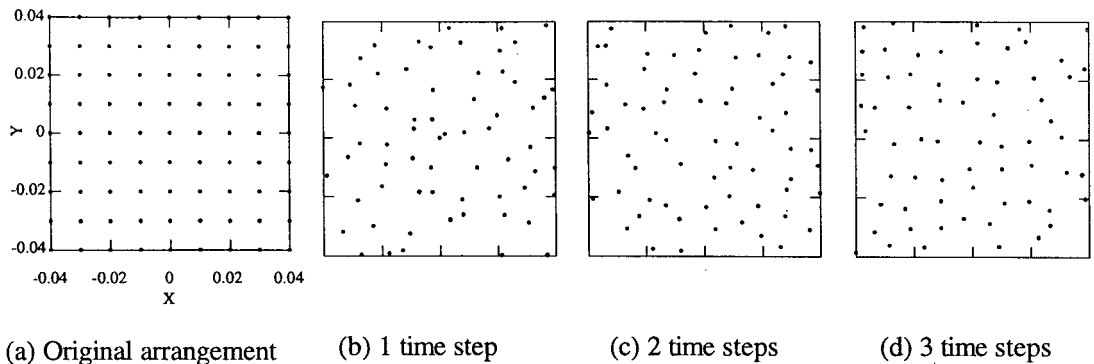
Figure 15. Randomly fluctuating calculation points.
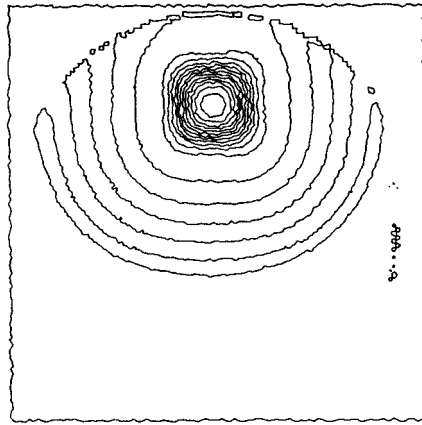
Figure 16. The result in the case of randomly fluctuating calculation points ($\Delta t = 0.005$).

marching method is applied to the conventional mesh-based upwind scheme including the CIP method.

3.1. Particle method and CNP method

The governing equation for particle movement is

$$\frac{\mathrm{d}x}{\mathrm{d}t} = u. \tag{16}$$

In the conventional particle method, the explicit evaluation (Equation (17)) and the implicit evaluation (Equation (18)) of Equation (16) are used.

$$x_i^{n+1} \cong x_i^n + \Delta t u_i^n. \tag{17}$$

$$x_i^{n+1} \cong x_i^n + \Delta t u_i^{n+1}. \tag{18}$$

However, since both the evaluation techniques have first-order accuracy in time, a large time step size in the case of a non-uniform flow will induce errors related to particle movement (see Figure 18). In order to solve this problem, the Crank–Nicolson-type particle movement evaluation method (CNP) is used,

Figure 17. The most deformed triangle used for the interpolation.
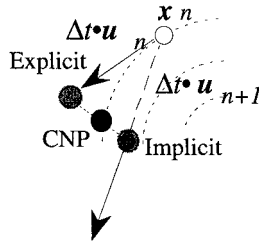
Figure 18. Comparison of particle movement evaluation schemes in the rotational field.

$$x_i^{n+1} \cong x_i^n + \Delta t \frac{u_i^n + u_i^{n+1}}{2}. \tag{19}$$

In addition to the CNP method, other higher-order time marching schemes, such as the Adams–Bashforth and Runge–Kutta methods, can also be used. For example, the second-order Adams–Bashforth scheme is given by

$$x_i^{n+1} \cong x_i^n + \frac{\Delta t}{2}(3u_i^n + u_i^{n-1}). \tag{20}$$

Here, the validity of above mentioned method is checked with the IAHR benchmark convection–diffusion problem [13]. The details are shown in Figure 19. The governing equation of this problem is

$$\frac{\partial f}{\partial t} + \boldsymbol{u} \cdot \nabla f = \underbrace{\frac{1}{Pe} \nabla^2 f}_{(D)}, \tag{21}$$

where Pe is the Peclet number. In order to use the CIVA-based method for solving Equation (21), the following equations are used as the governing equations for the spatial derivatives f^x and f^y:

$$\frac{\partial f^x}{\partial t} + \boldsymbol{u} \cdot \nabla f^x = -\boldsymbol{u}^x \cdot \Delta f + \underbrace{\frac{1}{Pe} \nabla^2 f^x}_{(D)}, \qquad \frac{\partial f^y}{\partial t} + \boldsymbol{u} \cdot \nabla f^y = -\boldsymbol{u}^y \cdot \Delta f + \underbrace{\frac{1}{Pe} \nabla^2 f^y}_{(D)}. \tag{22}$$

The part underlined (D) in Equation (21) represents the diffusion of the scalar quantity, while the parts underlined (D) in Equation (22) represent the diffusion effect of the derivatives. The other terms are the same as those of the problem in Section 2.4 and can be estimated by the same procedure as described in Section 2.4. To evaluate the diffusion terms (D) of the scalar quantity and the derivatives, the Laplacian model introduced by Koshizuka [6] is extended and a model that distributes not only the scalar quantity but also the derivatives is developed (see Figure 20).
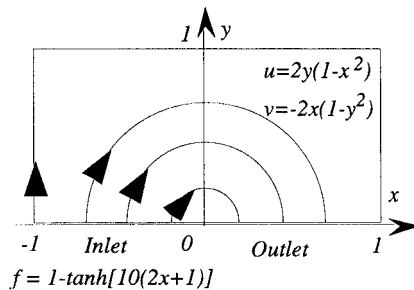
Figure 19. IAHR benchmark problem [13].
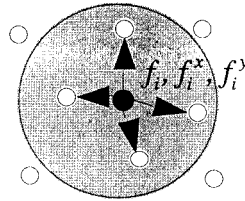
Figure 20. Diffusion model.

The scalar distribution at the outlet is compared in Figure 21, which includes the benchmark solution [14], the solution with the first-order interpolation and the solutions obtained by the explicit method and the implicit method combined with the CIVA method. Although there is little difference between the results for the first-order interpolation and the CIVA method at low *Pe*, the numerical viscosity for the CIVA method is smaller than those for the others at high *Pe* number. As predicted from Figure 18, the distribution obtained by the explicit method shifts away from the rotation center and that obtained by the implicit method shifts towards the rotation center. The CNP method is found to be the most accurate of the time marching methods for particle movement.

3.2. Application to the Godunov-type upwind scheme (including the CIP method)

The CNP method for particle movement is also applicable to the mesh-based upwind scheme including the CIP method. The evaluation of the convection term in the Godunov upwind scheme is described more correctly than in Equation (14) as

$$f(\boldsymbol{x}_i, t + \Delta t) \approx f(\boldsymbol{x}_i - \Delta t \boldsymbol{u}_i^n, t). \tag{14'}$$

The upwind scheme of Equation (14′) can also be explained as the downward movement of virtual (pseudo) particles according to the flow, which is shown in Figure 22. The differences between the CIP method and the CIVA–particle method are the same points of (A) and (B)

(A) Pe=10

(B) Pe=10^6
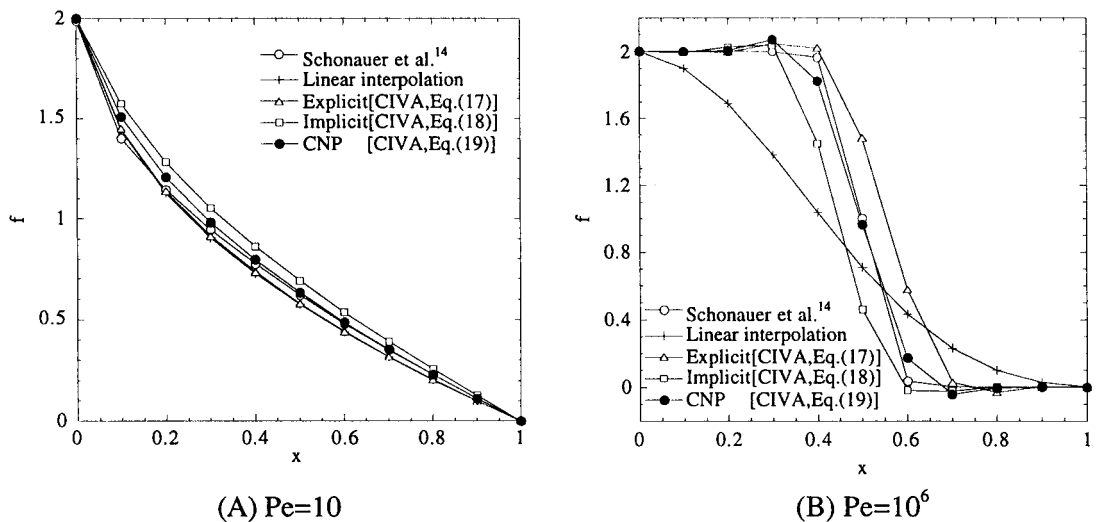
Figure 21. Comparison of scalar profiles at the outlet ($Cr = 0.8$).
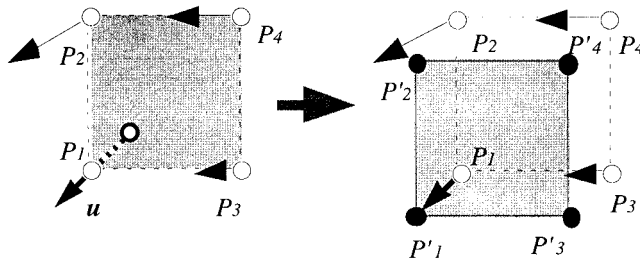
Figure 22. Godunov-type upwind scheme (left) and explanation using the concept of virtual particle movement (right).

as in Section 2.4. The CIVA–particle method is superior to the CIP method, because the CIVA–particle method takes the above points into consideration. Therefore, the CNP method is also applicable to position evaluation (virtual particle movement) in the Godunov method (see Figure 23). The evaluation in Equation (14′) used in the CIP method can be considered to be an explicit scheme. On the other hand, the following evaluation is considered to be an implicit scheme (Figure 23),

$$f(\boldsymbol{x}_i, t + \Delta t) \approx f(\boldsymbol{x}_i - \Delta t \boldsymbol{u}_i^{n+1}, t). \tag{23}$$

The scheme used in the GSMAC–CIP method proposed by Kaneyama and Tanahashi [15] is based on this implicit scheme. However, these two methods have first-order accuracy in time and induce errors in position evaluation in the same manner as in the case of the particle method (Figure 23). The author, therefore, applies the Crank–Nicolson-type evaluation scheme (CNP),

$$f(\boldsymbol{x}_i, t + \Delta t) \approx f\left(\boldsymbol{x}_i - \Delta t \frac{\boldsymbol{u}_i^n + \boldsymbol{u}_i^{n+1}}{2}, t\right), \tag{24}$$

to the original CIP method in order to improve the time integral accuracy.

The validity is checked using the same IAHR benchmark problem as in Section 3.2. At first, the results for the UTOPIA and CIP methods are compared in Figure 24 in the case of $Cr = 0.6$ (Cr is the Courant number). From the results for the CIP method, it can be confirmed that for the CIP method the result in the case of a steep slope is equivalent to that of the benchmark solution, but there is a marked difference in the position of the steep slope. On the other hand, with UTOPIA, it is confirmed that the overshoot is large and the slope is gentler than that obtained by the CIP method, but there is less difference in the slope position than for the CIP method. Next, the performance of the CIP method was analyzed by changing time step size. The result is shown in Figure 25. It is found that to achieve the same accuracy as the
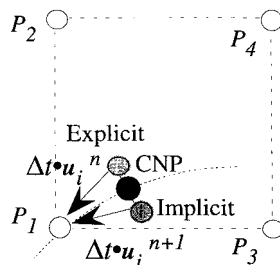
Figure 23. Comparison of upwind schemes in the rotational field.
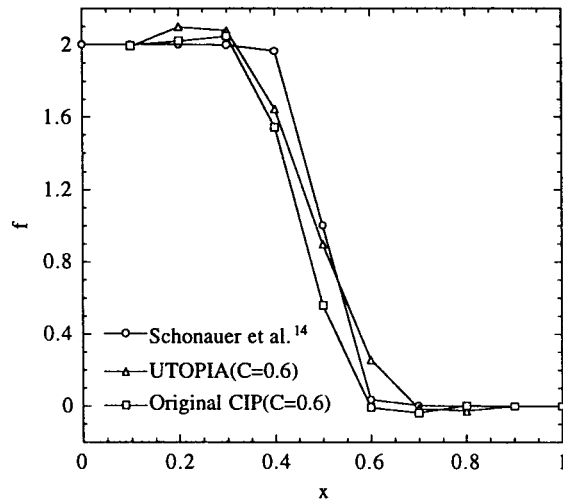
Figure 24. Comparison of CIP with UTOPIA.

benchmark solution, it is necessary to reduce the Courant number to about 0.2 or 0.02 when using the CIP method. It is thought that this error in position originates in the low accuracy of the explicit evaluation of position (Equation (14′)). Therefore, the distribution of the solution shifts in the direction of the rotation center as predicted from Figure 23. In order to improve accuracy of position evaluation, the CNP method was integrated into the CIP method. The result of $Cr = 0.6$ is shown in Figure 26, which includes the results obtained by the implicit evaluation for comparison. In the implicit method, the solution shifts away from the rotation center as predicted. From the results, it can be confirmed that the implicit CIP method proposed by Makuuchi et al. [16] causes the same problems in multi-dimensional non-uniform flow because the implicit scheme may use a larger time step size than the explicit scheme. On the other hand, despite the large Courant number, the result for the CNP method
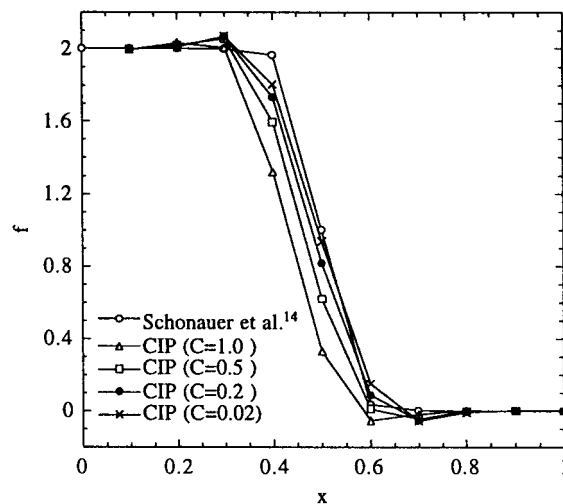
Figure 25. Effect of variation of the time step on the results with CIP.
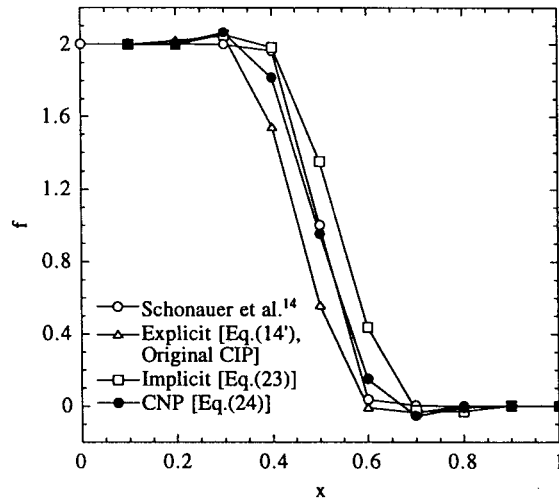
Figure 26. Comparison of the results obtained using three different evaluation methods for particle movement ($Cr = 0.6$).

is found to have the same accuracy as that for $Cr = 0.02$ in the case of the explicit method, and the accuracy with respect to time is thus improved.

4. CONCLUSION

A simple, efficient, flexible and accurate interpolation method, CIVA, was introduced for mesh-free algorithms for flow simulations. The CIVA method utilizes the concept of the CIP method and enables mesh-free cubic interpolation in a tetrahedron for three dimensions and in a triangle for two dimensions. By using the local or natural co-ordinate system, such as volume and area co-ordinates, the CIVA method solves the problems that are generally caused by the mesh-free cubic interpolation in those forms. New accurate mesh-free methods, such as the CIVA–gridless method and the CIVA–particle method were developed from the CIVA method. In particular, the CIVA–particle method, which consists of Lagrangian, rearrangement and interpolation steps, is flexible in the treatment of moving calculation points. Thus, the method enables integration of the gridless method, the particle method and the CIP method. Using a pure convection problem as a benchmark, the CIVA-based mesh-free method was found to be stable and to cause little numerical viscosity.

As it is important for the CIVA-based mesh-free method to correctly evaluate particle movement in order to achieve high accuracy, the evaluating algorithm was also improved by using a higher-order time marching scheme. The validity was confirmed using a convection–diffusion problem. The algorithm for evaluating particle movement was also made applicable to mesh-based conventional upwind schemes, including the CIP method, by interpreting the upwind scheme as virtual particle movement with the flow. From the computed results, the evaluating algorithm was confirmed to be effective for the conventional mesh-based method and to improve computational accuracy.

Since the CIVA-based mesh-free method has the advantage of the rearranged particle position being independent of the original position and the flow direction, it is applicable with sufficient accuracy to various types of methods. For example, Yoon *et al.* have applied this

LRI concept to the moving particle semi-implicit (MPS) method and succeeded in solving free-surface flow problems with inlet and outlet boundaries [17]. It is inherently impossible for the MPS method to solve problems with inlet and outlet boundaries because the particle number density cannot be kept constant. To solve the problem, the author's concept of the LRI algorithm was applied to the MPS method. This is a good example of the application of this method. Of course, the CIVA method is also useful for conventional mesh-based methods. It is thought that it will be effective to apply it to methods based on an unstructured mesh system in order to improve the computation accuracy. Consequently, the CIVA-based mesh-free methods will make it possible to perform highly accurate simulation for wide range of problems, including complicated geometries and complicated phenomena with various kinds of methods, because they enable flexible, efficient and accurate fluid simulations. In the future, it is intended to develop a mesh-free method that is applicable to more complex problems, such as the fluid–structure interaction, turbulent flow and multi-phase flow.

APPENDIX A. TRUNCATION ERROR OF THE CIP METHOD

The truncation error of the CIP method is examined here using the Taylor expansion. In the case of one-dimensional uniform flow, the algorithm to solve the convection problem with the CIP method can be expressed as

$$f_j^{n+1} = (c-1)^2(2c+1)f_j^n + c^2(3-2c)f_{j-1}^n - \Delta x c(c-1)^2 f_j'^n + \Delta x c^2(1-c)^2 f_{j-1}'^n, \tag{A.1}$$

$$f_j'^{n+1} = \frac{6}{\Delta x}c(1-c)f_i - \frac{6}{\Delta x}c(1-c)f_{j-1} + (1-c)(1-3c)f_j' + c(3c-2)f_{j-1}', \tag{A.2}$$

where $c = u\Delta t/\Delta x$, u is the uniform velocity, Δt is the time increment and Δx is the mesh interval.

Then, the relations

$$f_{j-1}^n = f_j^n - \Delta x f_j'^n + \frac{\Delta x^2}{2}\frac{\partial^2 f}{\partial x^2}\bigg|_j^n - \frac{\Delta x^3}{6}\frac{\partial^3 f}{\partial x^3}\bigg|_j^n + \frac{\Delta x^4}{24}\frac{\partial^4 f}{\partial x^4}\bigg|_j^n - O_1(\Delta x^5),$$

$$f_{j-1}'^n = f_j'^n - \Delta x\frac{\partial^2 f}{\partial x^2}\bigg|_j^n + \frac{\Delta x^2}{2}\frac{\partial^3 f}{\partial x^3}\bigg|_j^n - \frac{\Delta x^3}{6}\frac{\partial^4 f}{\partial x^4}\bigg|_j^n + O_2(\Delta x^4), \tag{A3}$$

$$f_j^{n+1} = f_j^n + \Delta t\frac{\partial f}{\partial t}\bigg|_j^n + \frac{\Delta t^2}{2}\frac{\partial^2 f}{\partial t^3}\bigg|_j^n + \frac{\Delta t^3}{6}\frac{\partial^3 f}{\partial t^4}\bigg|_j^n + \frac{\Delta t^4}{24}\frac{\partial^2 f}{\partial t^4}\bigg|_j^n + O(\Delta t^5),$$

and

$$\frac{\partial^2 f}{\partial^2 t} = -u\frac{\partial^2 f}{\partial t\,\partial x} = u^2\frac{\partial^2 f}{\partial x^2}, \qquad \frac{\partial^3 f}{\partial^3 t} = -u^3\frac{\partial^3 f}{\partial x^3}, \qquad \frac{\partial^4 f}{\partial^4 t} = u^4\frac{\partial^4 f}{\partial x^4} \tag{A.4}$$

can be established. By substituting the relations into Equation (A.1), we get

$$\frac{\partial f}{\partial t}\bigg|_j^n = -u\frac{\partial f}{\partial x}\bigg|_j^n - u\frac{c(1-c)^2}{24}\cdot\Delta x^3\frac{\partial^4 f}{\partial x^4}\bigg|_j^n + O(\Delta x^4, \Delta t^4). \tag{A.5}$$

Therefore, the CIP method is found to be a scheme that is third-order both in space and in time. Note that the derivative can be expressed as

$$\frac{\partial f'}{\partial t}\bigg|_j^n = -u\frac{\partial f'}{\partial x}\bigg|_j^n + u\frac{(1-c)(1-2c)}{12}\cdot\Delta x^2\frac{\partial^3 f}{\partial x^3}\bigg|_j^n + O(\Delta x^3, \Delta t^3). \tag{A.6}$$

However, the above discussion holds only for the case of one-dimensional uniform flow. In the case of two-dimensional non-uniform flow, the accuracy of the time integral deteriorates as described in Section 3.

REFERENCES

1. J.T. Batina, 'A gridless Euler/Navier–Stokes solution algorithm for complex aircraft applications', *AIAA Paper 93-0333*, 1993.
2. N. Satofuka, K. Morinishi and A. Nakao, 'Parallel implementation of gridless algorithm for computational fluid dynamics', in N. Satofuka, J. Periaux and A. Ecer (eds.), *Parallel Computational Fluid Dynamics*, North-Holland, Elsevier, 1995, pp. 349–356.
3. F.H. Harlow, 'The particle-in-cell method for fluid dynamics', in B. Alder, S. Fernbach and M. Rotenberg (eds.), *Methods in Computational Physisc*, vol. 3, Academic Press, New York, 1964, p. 319.
4. A.J. Chorin, 'Numerical study of slightly viscous flow', *J. Fluid Mech.*, **59**, 785–796 (1973).
5. J.J. Monaghan, 'An introduction to SPH', *Comput. Phys. Commun.*, **48**, 374 (1988).
6. S. Koshizuka and Y. Oka, 'Moving particle semi-implicit method for fragmentation of incompressible fluid', *Nucl. Sci. Eng.*, **123**, 421–434 (1996).
7. T. Yabe, T. Ishikawa and P.Y. Wang, 'A universal solver for hyperbolic equations by cubic–polynomial interpolation II. Two- and three-dimensional solvers', *Comput. Phys. Commun.*, **66**, 233–242 (1991).
8. T. Aoki, 'CIP advection on triangular mesh', *CIPUS Annual Report*, *CIPUS-A94*, Tokyo Institute of Technology on June 1, 1995, pp. 12–16.
9. N. Tanaka, 'High accuracy gridless algorithm and the application to particle methods', *Proc. JSCES Conf. on Computational Engineering and Science*, *No. 1-1*, *7-10*, 1996 (in Japanese).
10. N. Tanaka, 'Integration of the gridless, particle and CIP methods', *Proc. JSME 74th Spring Annual Meeting (V)*, *No. 97-1*, *10-11*, 1997 (in Japanese).
11. O.C. Zienkiewicz, *The Finite Element Method* (3rd edn.), McGraw-Hill, New York, 1977.
12. G.P. Bazeley, Y.K. Cheung, B.M. Irons and O.C. Zienkiewicz, 'The triangular elements in bending-conforming and non-conforming solutions', *Proc. Conf. Matrix Methods in Structural Mechanics*, Air Force Institute of Technolnogy, Wright Patterson AFB, OH, 1965.
13. R.M. Smith and A.G. Hutton, 'The numerical treatment of advection: a performance comparison of current methods', *Numer. Heat Transf.*, **5**, 439–461 (1982).
14. W. Schonauer, K. Raith and G. Glotz, 'The self adaptive solution of non-linear 2D boundary value problems in a rectangular domain', *Proc. Int. Conf. Numerical Methods in Laminar and Turbulent Flow*, Venice, Prineridge, 1981.
15. M. Kaneyama and T. Tanahashi, 'Numerical analysis of forced convection in a square cavity using GSMAC–CIP finite element method', *J. Jpn. Soc. Simul. Tech.*, **16**, (1997) (in Japanese).
16. H. Makuuchi, T. Aoki and T. Yabe, 'Implicit CIP (cubic-interpolated propagation) method in two dimensions', *JSME Int. J.*, **40**, 365–376 (1997).
17. H.Y. Yoon, S. Koshizuka and Y. Oka, 'A particle–gridless hybrid method for incompressible flows', *J. Numer. Methods Fluids*, in press.